Computational aspects of simulated migrated seismics for fast improved geological modeling

Gerrit Toxopeus[†] Kees Wapenaar[†], Steen Petersen[‡] and Jan Thorbecke[†]

[†]Department of Applied Earth Sciences
Delft University of Technology,
Mijnbouwstraat 120, 2628 RX Delft, The Netherlands
[‡]Norsk Hydro, research center, Bergen Norway
G.Toxopeus@CITG.TUDelft.nl

Abstract

A new method is presented which combines a forward and an image operator (resolution function) to construct a simulated migrated seismic section from a geological depth model. To efficiently use this tool during seismic interpretation, a fast implementation is necessary. This is achieved by improving the performance of the serial algorithm.

1 Introduction

The seismic experiment is an important tool for "understanding" the subsurface geology. A prerequisite for such an understanding is a clear relation between the seismic image and the complex Geological Depth Model. Let the collection of seismograms in general be given by the following representation:

$$\text{Data}(\mathbf{x}^R,\mathbf{x}^S,t)=$$
$$\text{Forward Operator }\{\text{Geological Depth Model}(\mathbf{x})\},$$

where Data denotes the recording of the (real or simulated) seismic experiment in time t, measured at position $\mathbf{x}^R$ due to a seismic source at location $\mathbf{x}^S$. The Forward Operator symbolizes either the seismic experiment in the field itself or stands for a computational procedure. To capture the geology from seismic measurements an Image Operator has to be applied

$$\text{Depth Image}(\mathbf{x})= \text{Image Operator }\{\text{Data}(\mathbf{x}^R,\mathbf{x}^S,t)\}.$$

The Depth Image should be representative for the Geological Depth Model. In the synthesis stage the geologist is concerned with the question how and to what extent geological details are visible in the seismic image. The following relation will be investigated

$$\text{Depth Image}(\mathbf{x})= \text{Image Operator }\{\text{ Forward Operator }\{\text{Geological Depth Model }(\mathbf{x})\}\},$$

which is the compound operation of the aforementioned processes. Commonly, the 1D convolution method ([1], [2] and [3]) is used to create synthetic seismics. However, the 1D (convolution) method only expresses the vertical resolution, while the combined operator also expresses the horizontal resolution of primary waves. Compared to other forward and migration schemes (e.g. based on finite differences, [4] and [5]) the compound operator considerably saves on computational time and storage, because we do not have to output the full intermediate 3D recordings $(\text{Data}(\mathbf{x}^R,\mathbf{x}^S,t))$. Together with geological modeling software this new method will provide the interpreter with a new powerful tool that helps to understand migration effects on a geological model. More specifically, due to its low computational costs, different geological models can be rapidly evaluated.

The objective of this paper is to carefully investigate the computational aspects of a serial implementation of the proposed method, in order to maximally aid the seismic interpreter. The paper is divided into two parts. The first part presents the new method, together with an example. The second part focuses on reducing the computational costs of the serial algorithm. Note that we will not deal with the question on how the actual comparison between the simulated migrated and real migrated seismics is performed.

2 Framework for combined operator

Figure 1 shows the framework to simulate a migrated seismic section. Input is a 3D (shared earth) geological depth model containing gridded wave velocities and rock density data. The framework can be
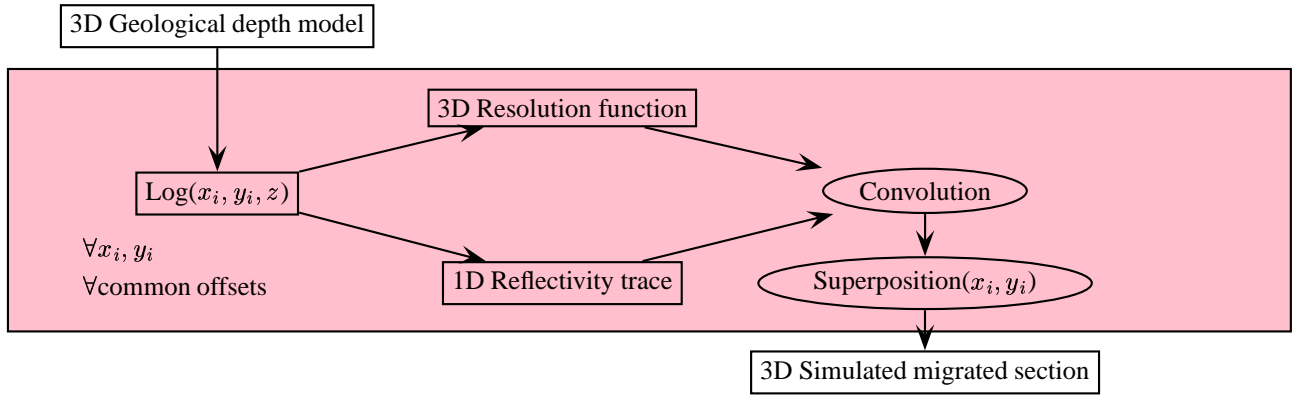
Figure 1: Framework to obtain a simulated migrated seismic section. Summarized by convolving the resolution function (upper flow) with a reflectivity trace (lower flow), followed by superposition of all convolution products for all reflectivity traces.

summarized by convolving the 3D resolution function (upper flow) with a 1D reflectivity trace (lower flow), followed by superposition of all convolution products for all reflectivity traces. The resolution function is the result of the combined operators and will be considered in more detail in the next section. In the convolution step the resolution function is assumed to be constant over a specific vertical range. The Zoeppritz equations are used to calculate the 1D reflectivity trace. If we restrict ourself to normal incidence waves (zero offset) the Zoeppritz equations reduce to

$$\text{Reflectivity}(z_i) = \frac{\rho(z_i)c(z_i) - \rho(z_{i-1})c(z_{i-1})}{\rho(z_i)c(z_i) + \rho(z_{i-1})c(z_{i-1})}, \tag{1}$$

where ρ is the mass density and c is the wavefield velocity.

3 Resolution function

The resolution function is acquired in two steps. First, the response of a scatterer is derived using a forward operator and the exploding reflector analogy (see Figure 2). Second, an image operator is applied, which results in a so-called resolution function or "focusing cross" ([6]). This section will concentrate on the mathematical aspects of both operators and show an example.

3.1 Gazdag phase shift operators

Let us consider the two dimensional version of the homogeneous acoustic wave equation

$$\nabla^2 p - \frac{1}{c^2}\frac{\partial^2 p}{\partial t^2} = 0, \tag{2}$$

where p=pressure, c=wavefield velocity and ∇^2 is the Laplace operator. Fourier transformation of (2)
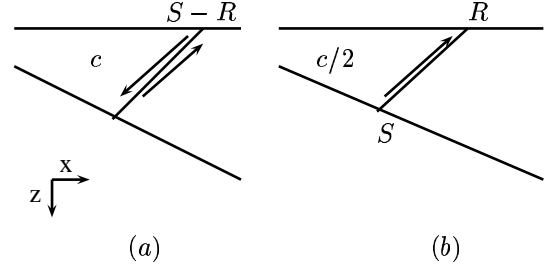
Figure 2: Recording data. (a) Seismic experiment which is performed in the field. (b) The exploding reflector analogy. The source is now placed at the reflector and half the velocity is taken to resemble the field experiment. c denotes wavefield velocity, S is a source and R is a receiver.

with respect to x, y and t yields the Helmholtz equation

$$\partial_z^2 \tilde{P} + (k^2 - k_x^2 - k_y^2)\tilde{P} = 0 \tag{3}$$

with $k = \frac{\omega}{c}$. In the exploding reflector model we take $k = \frac{\omega}{c/2}$. The solution to the Helmholtz equation (3) is well known

$$\tilde{P}(k_x, z, \omega) = \tilde{P}(k_x, z_m, \omega) \exp^{(\pm jk_z|z_m - z|)} \tag{4}$$

with $k_z = \sqrt{k^2 - k_x^2 - k_y^2}$. On physical grounds the minus sign is chosen for forward wave propagation. The plus sign is for backward or inverse propagation, an image operation. The forward operator shows that wave field propagation in a homogeneous layer can be described by a phase shift operator in the double Fourier domain or k_x, k_y, ω domain ([7]). The wave field extrapolation operator was introduced by Gazdag [8]. Since then, this method has been named the "Gazdag phase shift method".

The Gazdag phase shift is used in combination with the exploding reflector analogy (see Figure 2).

$$\tilde{P}^-(z_{m-1}) = \tilde{W}^-(z_{m-1}, z_m)\tilde{P}^-(z_m) \tag{5}$$

with $\quad \tilde{W}^-(z_{m-1}, z_m) = \exp^{(-jk_z|z_{m-1}-z_m|)}$

The inverse wave field extrapolator ($\tilde{F}^- = 1/\tilde{W}^-$) forms the basis for Gazdag phase shift migration. To obtain a stable inverse wavefield extrapolator, the complex conjugate of the forward operator is taken $<\tilde{F}^->= (\tilde{W}^-)^*$. Physically, this means that only the propagating wave region is used. Hence,

$$\tilde{P}^-(z_m) = <\tilde{F}^-(z_m, z_{m-1})> \tilde{P}^-(z_{m-1}) \quad (6)$$

with $<\tilde{F}^-(z_m, z_{m-1})> = \exp^{(+jk_z^*|z_m-z_{m-1}|)}$.

The final migrated image in the exploding reflector analogy is obtained when the wavefield is evaluated at $t = 0$. In the double Fourier domain this is a summation of all the frequencies components for each (k_x, ky, z). Finally, the image is inverse Fourier transformed from the wavenumber domain to the space domain

$$Image(x, y, z) = (FFT)^{-2}\left[\sum_{\omega_i} \tilde{P}(k_x, k_y, z, \omega_i)\right].$$
$$(7)$$

For more extensive details we refer to Berkhout [9] and Wapenaar [10].

3.2 Acquisition parameters

Figure 3 illustrates an acquisition setup. As an illustration for two different acquisition setups the influence on the representation of the resolution function will be considered for a 2D medium. In the model three equal-strength point scatterers are located at 500, 1500 and 2500 meters in a homogeneous medium with P-wave velocity of 2000 m/s. In the modeling, dz=2 and dx=5 meters. The source signature (Ricker wavelet) has a center frequency of 40 Hz. First we consider the acquisition setup with an "infinitely" large aperture and maximum propagation angle (α_{max}) of 90°. Figure 4 (a) shows that the resolution functions are nearly one-dimensional and can be interpreted as point scatterers convolved with the used wavelet. It is important to notice that the 1D convolution model would have given almost the same result. In the second more common acquisition setup, $\alpha_{max} = 60^o$ and the aperture width is limited to 3000 meters (see Figure 4 (b)). The 2D resolution functions are now "smeared" out compared to the first acquisition setup and vary with depth. This has two reasons: first, less angle information is available due to the maximum angle of propagation. Second, the limited aperture width makes the effective receiver array become smaller with increasing depth. As a consequence the deeper point scatterers have less angle information available and thus less spatial resolution.
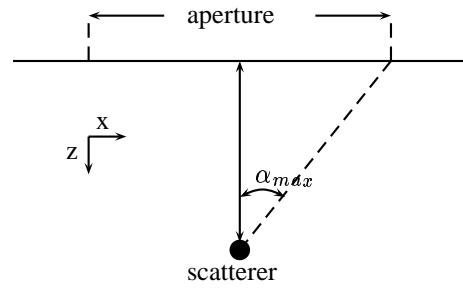
Figure 3: Acquisition setup with a limited aperture and selection of the maximum angle of propagation (α_{max}).
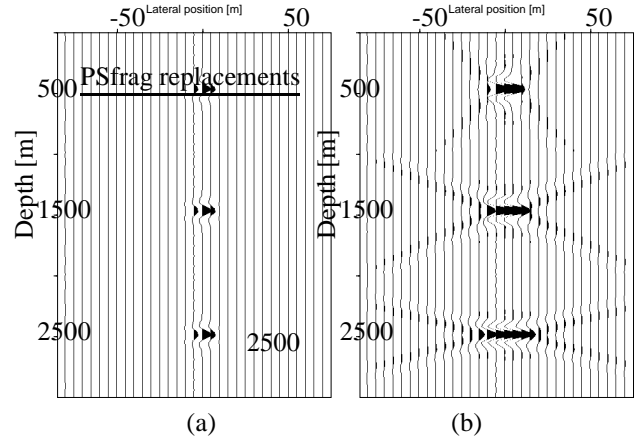
Figure 4: Resolution functions. Note that for display purposes the z-axis is reduced. (a) Recording "infinite" aperture and all propagation angles. Note that almost the same result would be obtained with the 1D convolution model. (b) $\alpha_{max} = 60^o$ together with an aperture width of 3000 meters. The 2D resolution function is "smeared" out and varies in depth.

3.3 2D Example

Figure 5 shows the Sigsbee2A synthetic dataset, which models the geologic setting found on the Sigsbee escarpment in the deep-water Gulf of Mexico. Notice the approximately 1000ft constant water layer on top of the model. This model is used to create a simulated migration section (see Figure 8). For comparison acoustic finite difference modeled shot records ([4]) are pre-stack depth migrated, Figure 9. Of importance is to notice that the latter seismic section is computed on a single CPU in approximately 1 week and requires approximately 550 Mb to store the intermediate shot records. On the other hand, the simulated migrated section is constructed in approximately 10 seconds (see Table 1 and discussion in next section) and requires no intermediate disk-space. Nowadays interpretation of seismic data is performed in three dimensions, where commonly an interpreter
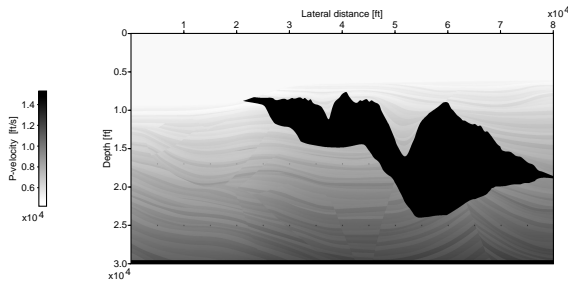
Figure 5: Sigsbee numerical dataset, models the geologic setting found on the Sigsbee escarpment in the deep water Gulf of Mexico.

Figure 6: Overview of the double Fourier domain. To reduce computational costs only the filled region is computed.

is helped by a large variety of (3D) attributes to understand the seismic data (see e.g. for a recent case study Luchford [11]). However, high computational costs of realistic forward seismic modeling (e.g. including migration effects) currently limit an interpreter to use a geological depth model to understand or justify seismic data during interpretation. However, using the proposed method combined with proper geological modeling software (e.g. [12]) this could change. The comparison of the real and simulated data may as well be extended to include the comparison of equally derived attributes of the migrated sections. The interpreter may use this attribute comparison to further understand the geology and adjust the model according to the attribute comparison.

4   Fast serial implementation

From the previous discussion it has become clear that a fast implementation is beneficial to aid the work of an interpreter. Due to the zero-offset restriction the calculation of the reflectivity (equation 1) is rather straightforward. Therefore, we focus on a fast implementation to obtain resolution functions from one log of the geological depth model. The implementation is done in the double Fourier domain on a RISC architecture. Note that we assume that we use the fastest available Fourier transform (FFTW) and that that the given analysis is presented for two dimensions, however the method is valid for three dimensions.

4.1   Double Fourier domain

Figure 6 shows the double Fourier or (k_x, ω) domain, where equation 4 is numerically solved. The horizontal axis displays the wavenumber (k_x) and the vertical axis the frequency $(\omega = 2\pi f)$. For an efficient implementation for both the forward and migration algorithm, consider the following four properties of equation 4. First, recognize that the Fourier transform is computed from a real and causal signal.
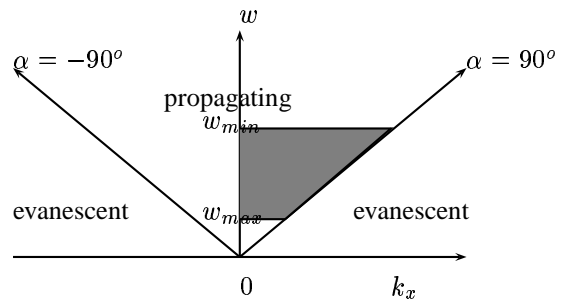
This means that only the positive frequencies have to be calculated, the real Fourier transform takes care of the negative values. Second, in the Helmholtz equation, k_x is squared. This means that it is symmetric in k_x and therefore only the positive part has to be calculated, the negative part is an exact copy. Third, if the square root of the phase shift operator becomes complex the wave field is evanescent (exponentially decaying). Therefore, the phase shift operator is only applied if the wavefield is propagating. And fourth, the available frequencies, which carry information, are limited. This means that in the frequency range up to Nyquist, not all frequencies need to be calculated. These four properties are shown as the filled region in Figure 6. Properties one to three are implemented in the "original" algorithm. To benchmark performance increase, one velocity log of the Sigsbee2A model (Figure 5) is taken. Table 1 shows the runtime of the "original" algorithm. To benchmark the performance increase for the fourth property the program is run with a realistic limited frequency range of 0 up to 60 Hz, instead of up to 100 Hz (Nyquist). Table 1 shows the performance increase. To further understand how to reduce the computational costs, the next subsections examine the individual parts.

4.2   Forward evaluation

Below is the pseudo code of the forward part (equation 5):

```
for z=nz to 1
  for w=wmin to wmax
    for kx=1 up to propagation limit
        check if depth point scatterer
        calculate phase shift operator
        apply phase shift operator
    end
  end
 apply filters
 copy symmetric kx part
end
```

Note that due to the exploding reflector analogue (see Figure 2) the depth loop is reversed. This straight forward implementation results in speedup after recognizing that the phase shift operator is a linear operation for constant velocity intervals. Constant intervals exist, for example due to a constant water layer (see Figure 5) or a constant taken overburden. The computational costs from finding the constant velocity intervals is negligible. Table 1 shows the computational speedup.

4.2.1 Acquisition

During modeling the characteristics of the acquisition setup (see Figure 3) are included by applying symmetric filters, which are briefly considered. Following Cerjan [13] the limitation of the aperture is archived by multiplying one side of the wavefield by a Gaussian shaped spatial function in the ω, x domain. This means that before and after applying this filter, a 1D Fourier transform from k_x to x is applied. To limit the maximum angle of propagation greater than α_{max}, (see Figures 6 and 3) a mask is designed to attenuate in the $k - \omega$ domain. Unfortunately, the dip-mask must be recalculated at every iteration because the frequency corresponding to a given dip changes as $k = \frac{k_x}{\sin \alpha}$. A so-called Hann-function, a raised-cosine, is used as dip filter.

4.3 Migration

The pseudo-code of the migration part, equations 6 and 7, respectively, is:

```
for z=1 to nz
  for w=wmin to wmax
    for kx=0 up to propagation limit
        calculate phase shift operator
        apply phase shift operator
    end
    sum over all frequencies
  end
 copy symmetric kx part
 inverse FFT
end
```

After carefully inspecting the program code, the k_x and ω loop were reversed. This was done because we overlooked the fact that we have defined w as the fastest dimension. Due to this cache optimization a 17 % performance increase is obtained (see Table 1).

4.4 Profiler

To further increase the computational performance of the serial algorithm, the GNU profiler (gprof) is used. The profiler shows that the main loops of the forward and migration algorithm are the most compute intensive parts of the program. Unfortunately the

	Runtime [s]
Original algorithm	197.4
Reducing frequencies	109.1
Using linear operator	12.4
Changing loop order	10.0

Table 1: Summarizing different serial improvements. C program compiled on Red-Hat 7.0 with Linux Intel compiler 6.0 and compile option -03.

profiler does not reveal this line by line. However examining the pseudo codes and equation 4, we have the following suggestions. First, the square root is present in both inner loop. And as the "Square Root page" [14] discusses, optimized versions of the square root operation are available. However, a listed optimized square root code (fsqrt) did not show any significant performance increase. Second, the exponential function (implemented as cosine and sine) could by replaced by a lookup table, to speed it up. Third, the division of ω and c could be replaced by multiplication, if first the reciprocal of c is taken. There already half the input velocity is computed (exploding reflector analogy), the reciprocal operator can be efficiently implemented. Finally, by vectorization, one loop is saved. Notice that we think that parallelization of the serial code, for example by frequency components, will not speedup the algorithm due to the parallelization overhead.

5 Parallelization

Parallelization of the framework (Figure 1), using as basis the optimized serial algorithm, is useful if from every log position (x_i, y_i) different resolution functions need to be computed or if different offsets are selected. For parallelization, the master-slave topology is adapted, where the master distributes the grid parameters (MPI_Bcast) to the different slaves. Each slave then computes a part of the final simulated migrated section, using the improved serial algorithm. In the end, the master collects (MPI_Receive) and superimposes the final simulated migrated image from all nodes. Only attention has to be paid that the slaves send (one operator length) extra information from their local convoluted result, because otherwise the "parallel" superposition performed by the master node is incorrect. Figure 7 shows the obtained speedup using the complete Sigsbee model. The result is almost linear. Note that the current implementation is only efficient for a homogeneous network, there the input grid is equally divided over the number of available slaves. It is better to follow the approach suggested by Dongarra, et al [15], where a random factor is introduced to determine the computed grid size for the slaves. When a slave is ready it requests
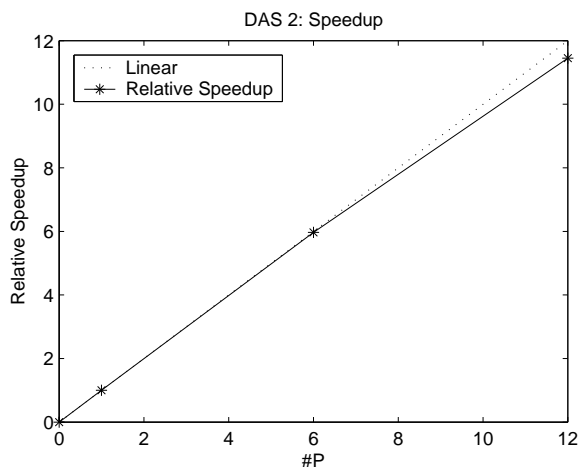
Figure 7: Obtaining an almost linear relative speedup on the DAS-2 cluster.

the next number of logs to be calculated.

6 Discussion

The above discussion provides a fast implementation for a new seismic simulation method, which includes migration effects. A fast implementation is necessary to optimal aid the work of a seismic interpreter. The serial code is optimized by carefully examining the properties of the double Fourier domain, physics and cache optimization. The speedup after optimization compared to the original algorithm is huge: 200 %. Note that the computational improvement can decrease if a log lacks constant velocity intervals or if higher frequencies are needed. Use of the GNU profiler (gprof) unfortunately did not reveal which lines in the code are a target for computational improvement. Our guess with an improved version of the square root, did not show any performance increase. Further targets are the exponential function or even vectorizing the code. Finally, a parallel implementation is beneficial if for every log position new resolution functions are calculated or different offsets are selected. An almost linear speedup is achieved.

Acknowledgment

References

[1] O. Yilmaz. *Seismic Data Processing*, page 526. Soc. of Expl. Geophys., 1987.

[2] O.M. Badescu. *Thick-bedded deep marine sandstones, the use of analogs for reservoir appraisal*. PhD thesis, TUD, 2002.

[3] L.F. Pratson and G. Wences. Seismic simulations of experimental strata. *AAPG*, 86(1):129–144, January 2002.

[4] G. Toxopeus, J.T. Fokkema, J. Groenenboom, and H.X. Lin. 3-D Parallel Elastic Finite Difference Wave Modeling. *Proceedings of the 8th annual conference of the Advanced School for computing and Imaging,Lochem, Netherlands*, 2002.

[5] D. Gavrilov, L. Lines, C. Bland, and T. Kocurko. 3-D depth migration: Parallel processing and migration movies. *The Leading Edge*, pages 1282–1284, December 2000.

[6] A.J. Berkhout. *Seismic resolution*. Seismic exploration. Geophysical press, London-Amsterdam, 1984.

[7] R.H. Stolt. Migration by Fourier transform. *Geophysics*, 43(1):23–48, 1978.

[8] J. Gazdag. Wave equation migration with the phase-shift method. *Geophysics*, 43:1342–1351, 1978.

[9] A.J. Berkhout. *Applied Seismic Wave Theory*. Advances in Exploration Geophysics 1. Elsevier Science, Amsterdam, 1987.

[10] C.P.A. Wapenaar and A.J. Berkhout. *Elastic wave field extrapolation: redatuming of single- and multi-component seismic data*. Advances in Exploration Geophysics 2. Elsevier Science, Amsterdam, 1989.

[11] J. Luchord, R. Gras, and D. Fakorede. Reducing exploration and production risk by visualization and seismic classification: a case study from the North Sea. *First Break*, 20(11):677–685, November 2002.

[12] S. Petersen. *Compound modelling,a geological approach to construction of shared earth models*. EAGE, 1999.

[13] C. Cerjan, D. Kosloff, R. Kosloff, and M. Reshef. A nonreflecting boundary condition for discrete acoustic and elastic wave equations. *Geophysics*, 50:705–708, 1985.

[14] P. Hsieh. http://www.azillionmonkeys.com/qed/sqroot.html.

[15] J. Dongarra, G.A. Geist, R. Manchek, and V.S. Sunderam. Integrated PVM Framework Supports Heterogeneous Network Computing. *Computers in physics*, 7(2):166–174, – 1993.
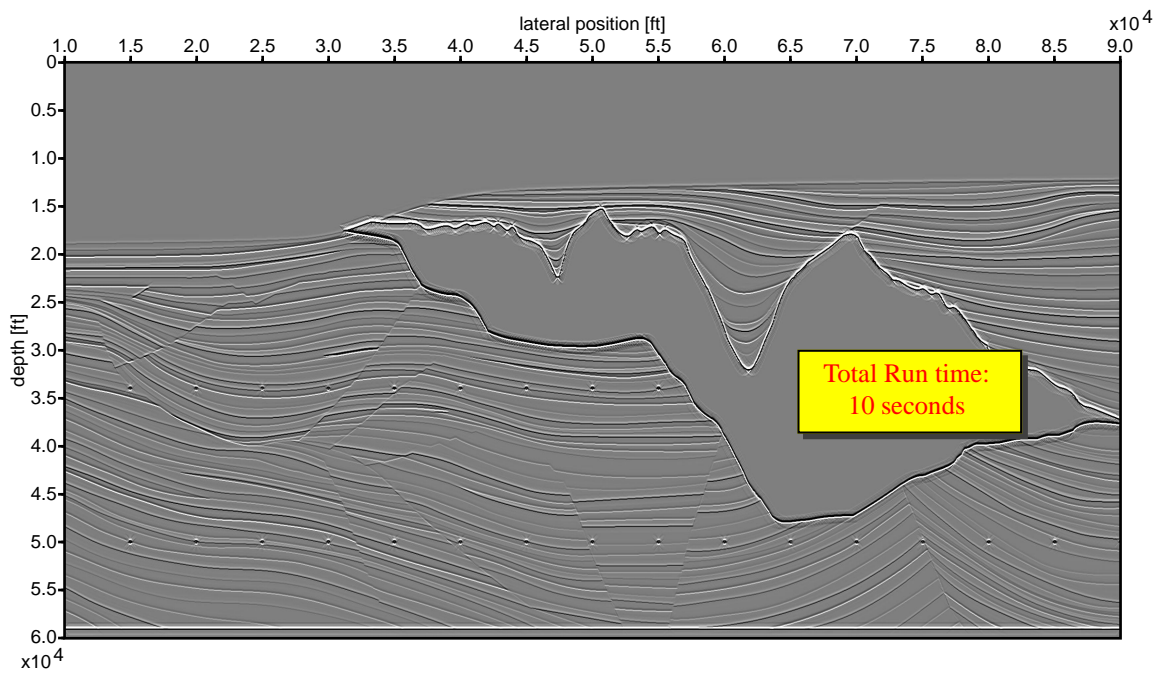
Figure 8: Migrated result of the Sigsbee data set using the presented method.
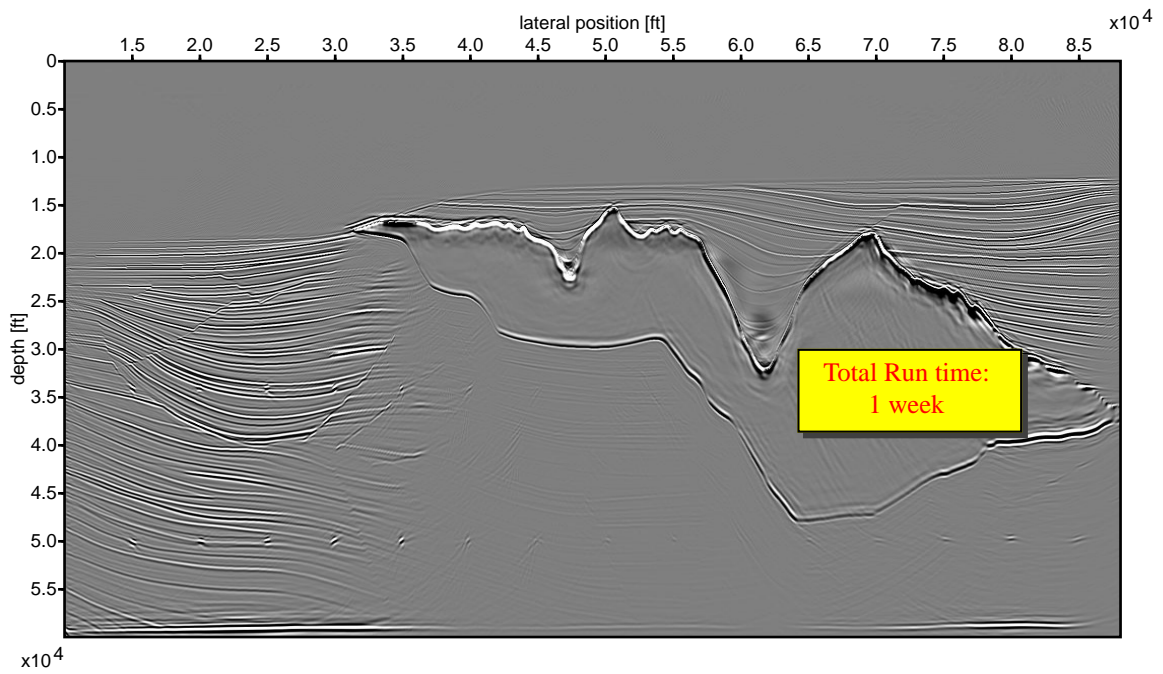
Figure 9: Migrated result of the Sigsbee data set using acoustic finite difference modeling of shot records and pre-stack depth migration.